Turbulent Flow Structure in Meandering Vegetated Open Channel

F. Jahra, H. Yamamoto, F. Hasegawa & Y. Kawahara
Department of Civil and Environmental Engineering, Hiroshima University, Higashi-Hiroshima, Japan

ABSTRACT: This study aims at revealing the flow structure of turbulent flows in a partially vegetated open channel where the width of vegetation zone changes as a sine-generated curve. The main objective of this paper is to gain insight into the mean flow field. Three-dimensional numerical simulation is carried out with the standard k-ε model to explore the distribution of mean velocity and turbulence structure in the main channel and the vegetation zone under both emergent and submerged vegetations. To capture the effect of vegetation on the flow, two different approaches have been adopted and the simulated results of these two approaches have been discussed. It is found that the second approach which has been developed in the field of meteorology has wide range of application to detect flow structure. The numerical results are compared against experimental observations in terms of mean velocities and Reynolds stresses, showing a fairly good agreement between simulated results and experimental results. The effect of change in vegetation density on flow structure is also discussed.

Keywords: *Vegetated open channel,3D k-ε model, flow structure, Reynolds stresses, emergent and submerged vegetations*

1 INTRODUCTION

Rivers and streams are usually in close association with vegetation. Natural rivers are mostly meandering and vegetation can occupy nearly every geomorphic position within the fluvial environment. Vegetations in and near streams are subjected to varying flow stages that can inundate vegetation during high flow events or leave it exposed during low flow events. Riparian vegetation can play a critical role in the physical, ecological, and hydraulic functions of streams and rivers. Vegetation can affect the transport of water, sediment, and nutrients both within the channel and to or between the riparian zones. The characterization of not only the mean flow, but also turbulence structure and the associated transport processes in presence of vegetation, has received a lot of attention in the last decade (Lopez & Garcia, 2001). Thus, the characteristic of turbulent flow over a vegetation layer is one of the most fundamental topics in hydraulics of flow with vegetation (Shimizu & Tsujimoto, 1994). The effect of marginal vegetation on flow resistance has been investigated for straight channels whereas

little is known of the effects for meandering channels under either inbank or overbank flow conditions (James & Myers, 2001). The insight into flow distribution in straight as well as meandering main channels and the neighboring vegetated area is indispensable in river management.

Mean flow and turbulence characteristics of open channel flow with vegetation have been studied through laboratory experiments and numerical computations. The k-ε model is the most commonly used two-equation model in engineering and has proved to be a reliable tool in a wide variety of problems in hydraulic and environmental engineering (Rodi, 1984). But none of the existing turbulence models are truly universal and thus, each model needs to be tuned to specific flows (Choi & Kang, 2004). Using the k-ε model, Shimizu & Tsujimoto (1994) simulated the vertical distributions of the development of mean and turbulent flow structures. Lopez & Garcia (1997) also computed flow structures of vegetated open channel and compared the calculated results with their experimental ones. Choi & Kang (2004) explained the performance of Reynolds stress model, algebraic stress model and the k-ε model for vege-

tated open channel flow simulation. Green (1992) modified a *k-ε* model to examine the air flow through and over an isolated stand of widely-spaced trees with PHOENICS computer program, where he introduced additional source and sink terms to account for the effect of forest stand on the adjacent flow field. Using the similar source and sink terms Liu et al. (1996) also simulated the turbulent flow field downwind of forest edge.

The present study shows an application of the standard *k-ε* model to calculate the three-dimensional flow structure of partially vegetated open-channel flow. Two different approaches have been introduced, conventional approach widely used in the field of river engineering and another approach used in field of meteorology to compute the effect of vegetation on the flow field. The governing equation is both the short time and spatially averaged and the effect of individual roughness elements has been taken into account by an averaged local drag force. The computed results have been compared with the laboratory measurement by the authors (Jahra et al., 2009) for two different vegetation densities and the values of model coefficients of both the models have been discussed.

2 EXPERIMENTAL SETUP

The experiments were conducted in a straight rectangular flume whose length and width are 22.0m and 1.82m, respectively. The channel has closed water supply system. Water is transported from downstream reservoir to the upstream reservoir by means of pipeline. The length of vegetation zone is 11.0m. The vegetation is idealized with wooden rigid cylinders of 3mm diameter and 5cm height. Three mean velocity components were measured by two-component electromagnetic current meters (both L-type and I-type) of 3mm diameter. Vegetation zones were prepared on either side of the channel in meandering shape to suppress the large scale vortices that may develop in straight shaped vegetation zone. The meandering wavelength is 2.2m with the sinuosity of 1.10. There are five complete waves along the 11.0m long vegetated zones. Two cases of experiment were carried out: a shallow water case where vegetation was emergent and a deep water case with fully submerged vegetation. The measurements were carried out at the downstream section (about 8.35m from the tailgate) over half wave length at the points *S1*=12.55m, *S2*=12.85m, *S3*=13.1m, *S4*=13.35m and *S5*=13.65m. The equations of the interface curves are $Z = 0.21\sin(2\pi x/l) + 0.435$ and

$Z = 0.21\sin(2\pi x/l) + 1.385$. Figure 1 depicts the measurement sections in the partially vegetated meandering channel. Figure 2 shows the layout of the flume. The channel geometry and the flow conditions are summarized in Table 1. Flume measurement has been carried out with two different vegetation densities, λ=0.13/cm and 0.033/cm, respectively.
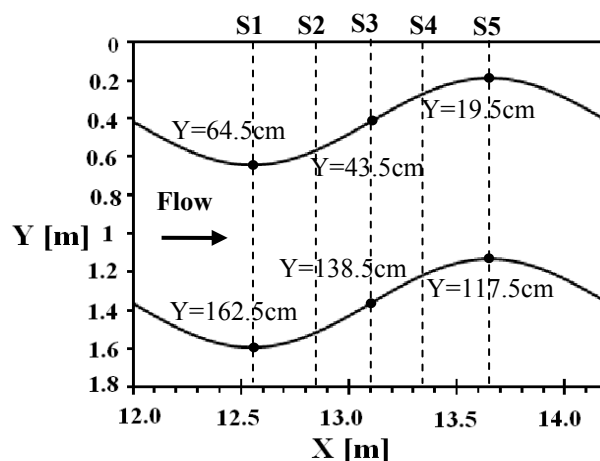

Figure 1. Measurement sections in meandering channel (plan view).

Figure 2. General layout of the meandering channel.

Table 1 Experimental condition for meandering channel.

Case	Bed slope	Discharge [l/s]	Flow depth [cm]	Vegetation density [1/cm]	Vegetation condition
A1	1/633	55.0	9.3	0.13	Submerged
A2			8.3	0.033	
B1	1/633	18.5	4.3	0.13	Emerged
B2			4.2	0.033	

3 MATHEMATICAL MODEL FORMULATION

The numerical calculations were conducted using the standard *k-ε* model. The computer code calculates hydrodynamics for three dimensional geome-

try. Here averaged equations in short time and space dimensions have been used. The vegetations are uniformly distributed on either side of the channel in meander form with the adjacent vegetation stem distance l_x and l_y in x and y directions, respectively. In present study two approaches for predicting the effect of vegetation on the flow structure have been discussed, where the conventional approach has been termed as "Approach 1" and the approach proposed by Green (1992) in the field of meteorology is termed as "Approach 2". The basic equations with the standard k-ε model are as follows:

Continuity equation:

$$\frac{\partial U_i}{\partial x_i} = 0 \tag{1}$$

Momentum equation:

$$\frac{\partial U_i}{\partial t} + \frac{\partial U_i U_j}{\partial x_j} = g_i - \frac{1}{\rho}\frac{\partial P}{\partial x_i} + \nu\frac{\partial^2 U_i}{\partial x_j \partial x_j} - F_i - \frac{\overline{\partial u_i u_j}}{\partial x_j} \tag{2}$$

Reynolds stress component:

$$-\overline{u_i u_j} = \nu_t\left(\frac{\partial U_i}{\partial x_j} + \frac{\partial U_j}{\partial x_i}\right) - \frac{2}{3}k\delta_{ij} \tag{3}$$

Eddy viscosity:

$$\nu_t = C_\mu \frac{k^2}{\varepsilon} \tag{4}$$

The distribution of k and ε can be expressed by the following transport equations:

$$\frac{\partial k}{\partial t} + \frac{\partial U_j k}{\partial x_j} = \frac{\partial}{\partial x_m}\left[\left(\frac{\nu_t}{\sigma_k} + \nu\right)\frac{\partial k}{\partial x_m}\right] + P_{rod} - \varepsilon + S_k \tag{5}$$

$$\frac{\partial \varepsilon}{\partial t} + \frac{\partial U_j \varepsilon}{\partial x_j} = \frac{\partial}{\partial x_m}\left[\left(\frac{\nu_t}{\sigma_\varepsilon} + \nu\right)\frac{\partial \varepsilon}{\partial x_m}\right]$$
$$+ \frac{\varepsilon}{k}C_{\varepsilon 1}P_{rod} - C_{\varepsilon 2}\frac{\varepsilon^2}{k} + S_\varepsilon \tag{6}$$

Production of turbulent kinetic energy:

$$P_{rod} = -\overline{u_i u_j}\frac{\partial U_i}{\partial x_j} = \nu_t\left(\frac{\partial U_i}{\partial x_j} + \frac{\partial U_j}{\partial x_i}\right)\frac{\partial U_i}{\partial x_j} \tag{7}$$

Drag force due to vegetation per unit volume of water:

$$F_i = \frac{1}{2}C_D\lambda U_i|\vec{U}| \tag{8}$$

Source/or sink terms S_k for k:

In Approach 1:

$$S_k = C_{fk}F_i U_i \tag{9}$$

In Approach 2:

$$S_k = F_i U_i - 2C_D\lambda|\vec{U}|k \tag{10}$$

Source/or sink terms S_ε for ε:

In Approach 1:

$$S_\varepsilon = C_{\varepsilon 1}C_{f\varepsilon}\frac{\varepsilon}{k}F_i U_i \tag{11}$$

In Approach 2:

$$S_\varepsilon = \frac{3}{2}\frac{\varepsilon}{k}F_i U_i - 3C_D\lambda|\vec{U}|\varepsilon \tag{12}$$

$$C_D(\text{Re}_d) = -8.5*10^{-4}\,\text{Re}_d + 1.5; \quad \text{Re}_d = \frac{DU_i}{\nu} \tag{13}$$

where, C_D is drag coefficient, λ is vegetation density defined by $\lambda = \frac{D}{l_x l_y}$. For the present experimental vegetation layout, λ=0.033/cm and 0.13/cm, C_D =0.65~1.0 has been considered for submerged and emergent vegetations, using the imperial equation Eq. (13) suggested by Poggi et al. (2004). The model constants are (Rodi, 1984): C_μ=0.09, σ_k=1.0, σ_ε=1.3, $C_{\varepsilon 1}$=1.44 and $C_{\varepsilon 2}$=1.92. Approach 1 has adopted the model coefficients C_{fk}=1.0, $C_{f\varepsilon}$=1.33, theoretically obtained by Burke & Stolzenbach (1983) considering model calibration result.

The basic equations are discretized by Finite volume method. The convective term has been discretized by Power-law scheme and the SIMPLE algorithm has been used. Along the bottom and the side walls "wall function" technique has been applied. The wall boundary conditions for U, k and ε are applied at a point $Z=Z_p$ adjacent to the wall and in the log-law region. The region between point Z_p and the actual wall is related by the following relationship (Rodi, 1984):

$$\frac{U_p}{U_*} = \frac{1}{\kappa}\ln\left(E_r\frac{Z_p U_*}{\nu}\right), \quad k_p = \frac{U_*^2}{\sqrt{C_\mu}}, \quad \varepsilon_p = \frac{U_*^3}{\kappa Z_p} \tag{14}$$

where wall roughness parameter, $E_r = e^{\kappa A}\nu/U_* k_s$. The equivalent roughness height, k_s=1 mm and

$$A = 8.5 - 5.57\log_{10}[1 + (3.3057\nu/U_* k_s)] \tag{15}$$

At the inlet all variables are specified to have constant values whereas at the downstream end the longitudinal gradients of all variables are assumed to be zero. Free surface is treated as a symmetry plane.

According to Liu et al. (1996) the predicted turbulent kinetic energy was 100% larger than their experimental measurement when the second term on the right hand side of Eq. (10) was ignored.

Green's (1992) equation (Eq. (12)) for the source and sink term of ε has been modified in the present study as it is only an assumption where mixing length is considered locally invariant. An additional problem is that the second term on the right hand side considers only the reduction in the dissipation rate due to the reduction in k resulting from short-circuited energy cascade and does not include the increase in dissipation rate due to the reduction of turbulence mixing length (Liu et al., 1996). For present numerical model with meteorological approach the second term on the right hand side of Eq. (12) has been modified by multiplying factor 0.47 to obtain fair agreement with the experimental turbulent kinetic energy profile of Ghisalberti (2007). The association between experimental result of U-velocity and turbulent kinetic energy profile with the calculated one by two approaches are shown in Figure 3. A good agreement between two approaches is due to the similar distribution of ν_t although Approach 1 yields larger k and ε than Approach 2.
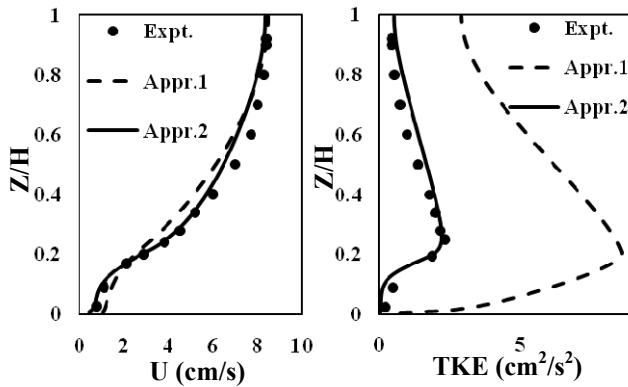

Figure 3. Profile of U-velocity (left) and turbulent kinetic energy (right). The canopy height is 8.3cm, i.e. 0.21H.

The present k-ε model is also found to reproduce all the cases of both the series R and A, simulated by Shimizu & Tsujimoto (1994), using both approaches.

4 EXPERIMENTAL AND NUMERICAL RESULTS

Flume experiment was carried out for both the submerged and emerged cases with two different vegetation densities to get a clear vision of the flow structure and these experimental results are compared with the simulated results of both the approaches.

4.1 Mean Flow and Turbulent Stresses for Submerged Vegetation

Flow in meandering cannel has complex behaviors. Figure 4(a) and Figure 4(b) show the U- velocity contours at the sections $S1$ and $S5$ respectively for both the experimental and calculated results of two different densities. It gives the qualitative view of the cross-sectional flow structure.
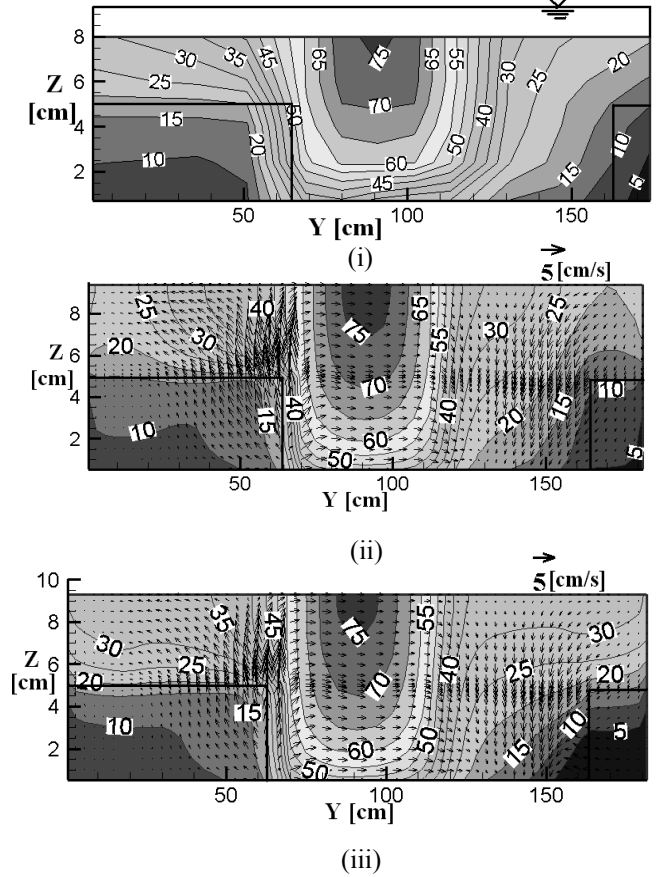

Figure 4(a). U-velocity (cm/sec) contour of submerged vegetation for Case A1, at section $S1$, (i): Experimental result, (ii) Calculated result of Appr. 1, (iii) Appr. 2.
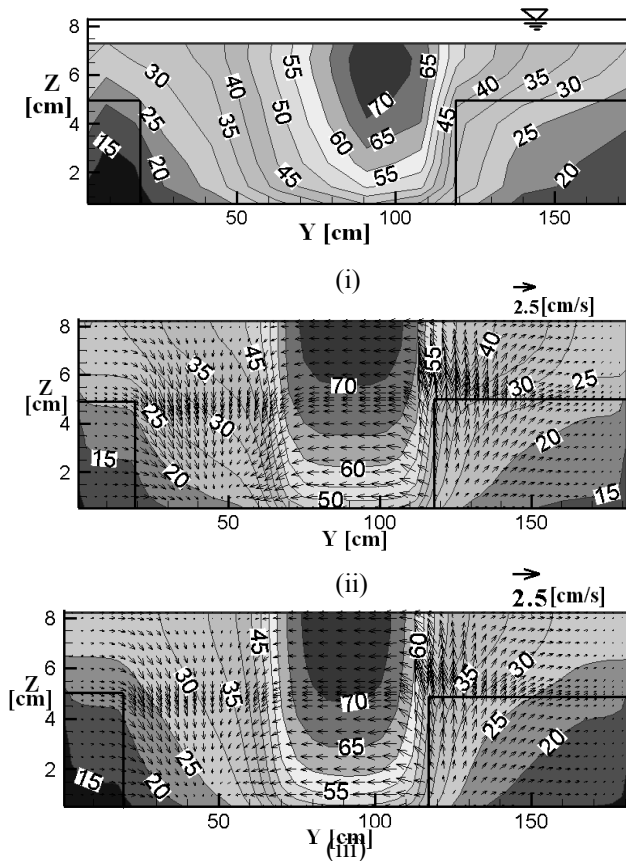
(i)

(ii)

(iii)

Figure 4(b). *U*-velocity (cm/sec) contour of submerged vegetation for Case *A2*, at section *S5*.

The maximum velocity region of primary velocity *U* is shifted toward the inner curve side, which can be explained by the pressure-driven *V*-velocity over water depth. It can be observed that both the approaches have a fair agreement with experimental result. Approach 2 can predict the flow within vegetation zone and in the main channel quite satisfactorily. In conventional approach both the k and ε are over estimated than the second approach. Although both the methods differ in terms of turbulent kinetic energy and dissipation rate, the agreement in velocity profile can be explained by the similar distribution of eddy viscosity (Figure 9).

Upward motions can be observed along the interface of the main channel and the inner vegetation curve and in both approaches (Figure. 4(a)). The similar phenomenon can be observed at section *S5* in Figure 4(b). Examination of the budget of *W*- momentum equation reveals that the streamwise convective term and pressure gradient term are nearly in balance to generate this pressure-driven secondary current. Deceleration of streamwise velocity causes an upward flow circulation near the inner wave in the channel. A downward motion occurs at opposite side of the inner waves of the channel.

Figure 5 describes the *U, V*-velocity vector distribution at *Z*=5cm. It has been observed that inner apex has higher velocity than the outer one and the velocity vector directs toward the main channel from the inner curve. Similar phenomenon was also observed by flow visualization.

Figure 6 shows the vertical *U*-velocity distribution for two different vegetation densities. The comparison has been made along the three measuring sections and at one measuring point, located in the meandering vegetated region. There is a good agreement between the calculated results with two different approaches and the flume measurement. With the change of vegetation density the qualitative as well as quantitative change in *U*-velocity profile can be observed. Spanwise distribution of simulated velocity profile also shows a good agreement with the experimental result.

The performance of the present numerical models has been tested concerning Reynolds stresses. Figure 7 and Figure 8 explain the vertical and spanwise distribution of Reynolds stresses, respectively. Spanwise distribution of Reynolds stress shows the profile of 5cm above the bed. It has been observed that the maximum positive and negative values of Reynolds stresses occur at the same position of the flume, i.e. at the interface of main channel and vegetated zone, which indicates the two inner curves of the left and right vegetation zone (considering half wave length). It indicates that the shear becomes dominant and the strongest along the inner curves in the main channel. It can be said that with the increase of vegetation density the Reynolds stresses increase. A good agreement between the two different models in terms of *U*-velocity as well as vertical and spanwise profile of Reynolds shear stresses can be observed due to the effect of similar distribution of eddy viscosity within the main channel and the vegetation zone. Although in Approach 1 both k and ε are over estimated (Figure 3), both the approaches show similar v_t profile, which is due to the ratio of k and ε in eddy viscosity. Figure 9 shows the vertical distribution of v_t within the vegetated area and at the interface of the main channel and the vegetation zone.

According to Choi & Kang (2004), for open-channel flows with submerged vegetation, RSM can predict the mean velocity and turbulence quantities better than algebraic stress model or the k-ε model. This limitation has been overcome in the present study.

4.2 Mean Flow and Turbulent Stresses for Emergent Vegetation

The flow structure has also been observed for emergent vegetations with different densities. Like submerged vegetation, emerged case also shows a reasonable agreement with the calculations by the two models. Figure 10 gives an image of the impact of change in vegetation density and also makes a qualitative comparison between laboratory experiment and numerical simulations. It has been observed that both the models could nicely represent the presence of vegetation, though in Approach 1 mean velocity was underestimated within the vegetation zone and overestimated in the main channel, especially near bed. This discrepancy can be explained by the concept of Choi & Kang (2004) and Tsujimoto et al. (1991), claiming that the drag-related weighting coefficients, C_{fk} and $C_{f\varepsilon}$ have to be tuned to specific flows. For Approach 1 these model coefficients in the present study have been calibrated with the submerged vegetation. Hence in case of emergent vegetation, another set of model coefficients should be introduced to obtain better results. Regarding drag-related weighting coefficients, Burke and Stolzenbach (1983) obtained theoretically C_{fk} = 1.0 and $C_{f\varepsilon}$ = 1.33. However, in numerical modeling, much smaller values for these coefficients were frequently used, for example, C_{fk} = 0.07 and $C_{f\varepsilon}$ = 0.16 by Shimizu & Tsujimoto (1994), and C_{fk} = $C_{f\varepsilon}$ = 0.0 by Fischer-Antze et al. (2001). It can be seen that the drag-related coefficients hardly affect the streamwise mean velocity and Reynolds stress profiles. However, these coefficients seriously affect the turbulence kinetic energy as well as turbulence intensity profile. This limitation of 3D k-ε model is overcome when Approach 2 has been implemented. The advantage of this approach is that without implementation of different sets of drag related model coefficients it can predict the flow structure quite satisfactorily for different vegetation densities under submerged and emergent vegetation conditions. Figure 11 shows the spanwise distribution of Reynolds shear stress. Here it can be observed that with the increase of vegetation density the spanwise Reynolds stress increases in terms of positive and negative along the two inner apex of the meandering wave. The calculated result has a reasonable agreement with the measurement.

Spanwise distribution of U-velocity can be observed in Figure 12. Both the measured and calculated points are located at 3.2 cm above the bed. Both the calculated results have a good agreement with the measured one. It can be observed that with the increase of vegetation density the velocity slope at the interface of main channel and the vegetation zone becomes steeper.
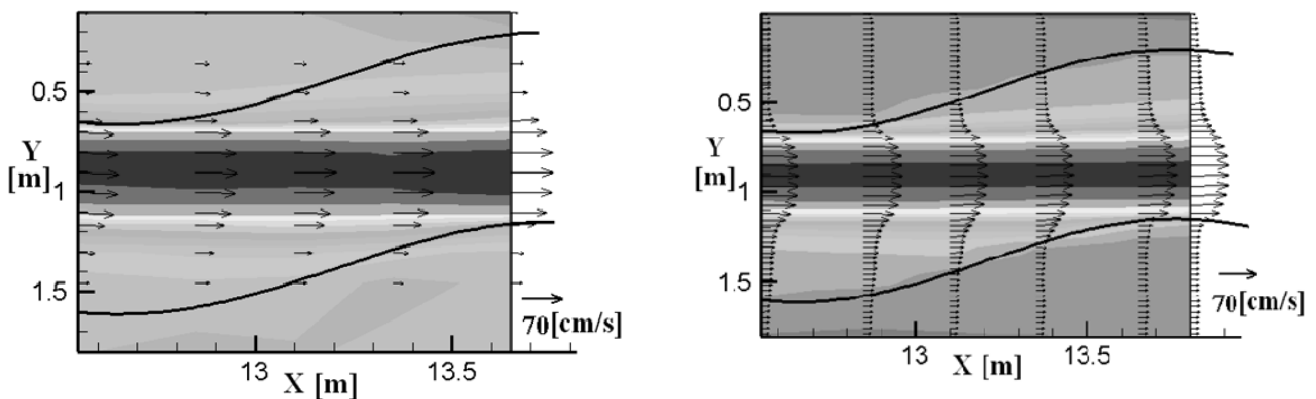

Figure 5. Distribution of U, V velocity vector of submerged vegetation for CaseA1, Left: Experimental result, Right: Calculated result by Approach 1.

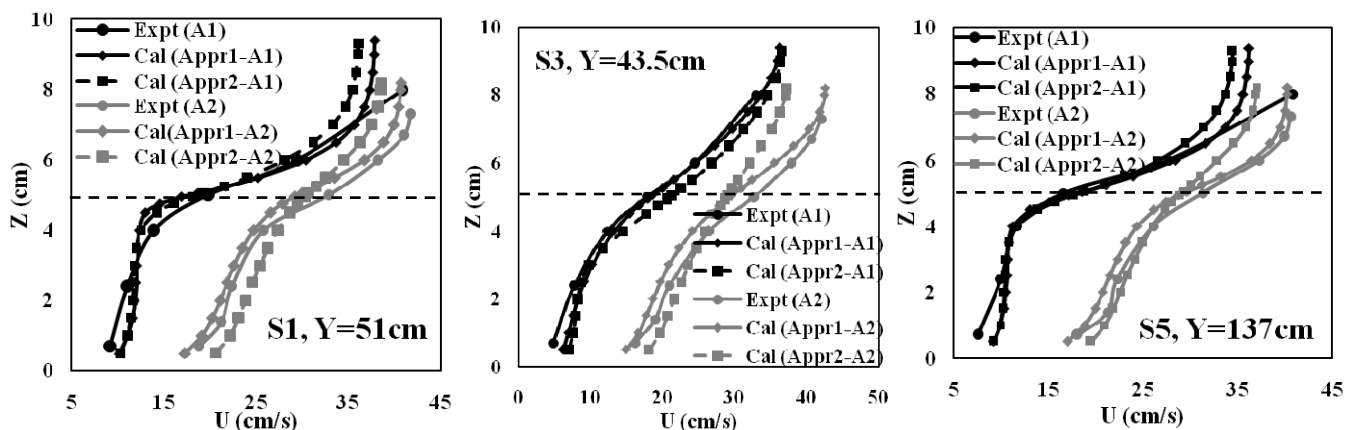
Figure 6. Experimental and calculated vertical distribution of U-mean velocity for submerged vegetation.
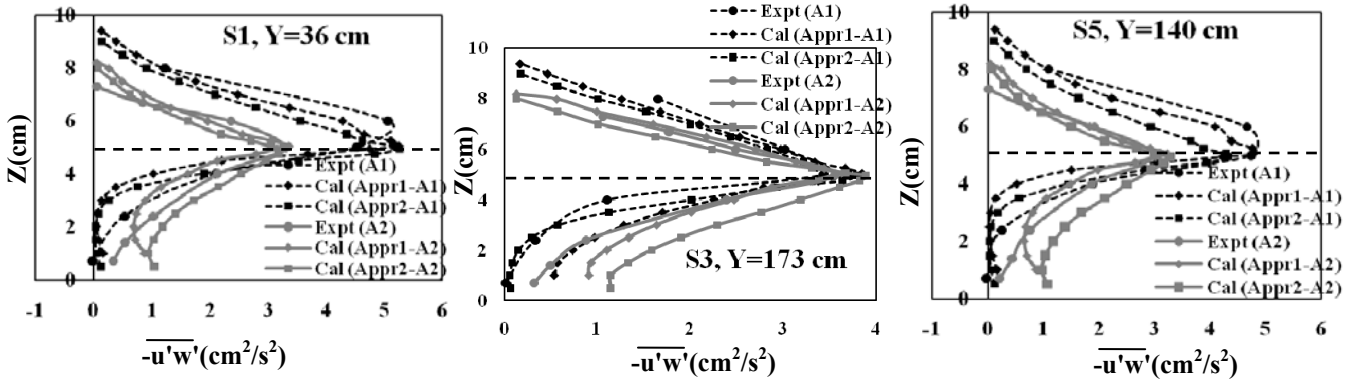
Figure 7. Experimental and calculated vertical distribution of Reynolds stress profile for submerged vegetation.
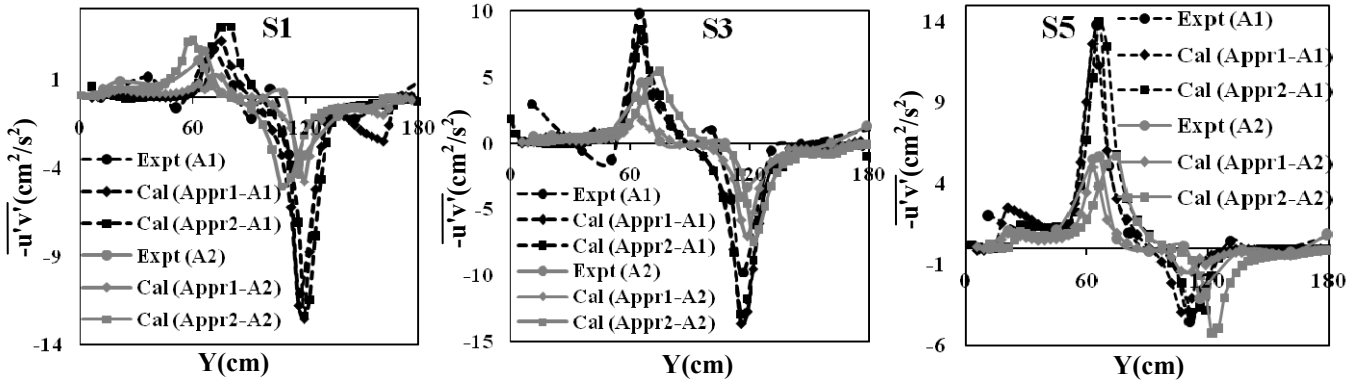

Figure 8. Experimental and calculated spanwise distribution of Reynolds stress profile for submerged vegetation.
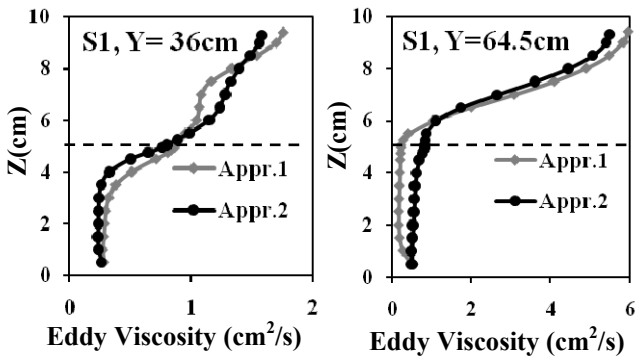

Figure 9. Profile of vertical distribution of Eddy viscosity of Case A1.

5 CONCLUSIONS

Flume experiments were carried out for turbulent open channel flows in the presence of meandering shaped vegetation under both submerged and emergent conditions. Numerical simulations were also performed with the standard k-ε model with the vegetation model in the transport equations for k and ε. The presence of vegetation has been introduced in the transport equations using two different approaches; the conventional approach and an approach used in the field of meteorology. Comparisons between the measured data and the numerical results have led to the following findings.

· The present k-ε models can reproduce the mean velocity field fairly well.
· The U-velocity increases in the main channel and decreases in the vegetation as the vegeta-

tion density increases, resulting in the increase in the vertical and spanwise Reynolds stresses at the vegetation interface.
· The maximum velocity region of U-velocity is shifted toward the inner wave due to the pressure driven secondary flows over water depth.
· Streamwise convective term and the pressure gradient produce upward and downward motions at the interface of the main channel and the vegetation zone.
· The present numerical model with conventional approach to detect the presence of vegetation can predict the flow structure for submerged vegetation satisfactorily, with some discrepancy in case of emergent vegetation. This infers that another set of model coefficients, C_{fk} and $C_{f\varepsilon}$ is needed for better agreement with the measurement for emergent vegetation. This limitation has been overcome by introducing new source/sink term in transport equations. Hence Approach 2 can be used for wide variety of flow filed with vegetation without any implementation of drag related model coefficients.

6 CONCLUSIONS

Flume experiments were carried out for turbulent open channel flows in the presence of meandering shaped vegetation under both submerged and

emergent conditions. Numerical simulations were also performed with the standard k-ε model with the vegetation model in the transport equations for k and ε. The presence of vegetation has been introduced in the transport equations using two different approaches; the conventional approach and an approach used in the field of meteorology. Comparisons between the measured data and the numerical results have led to the following findings.

· The present k-ε models can reproduce the mean velocity field fairly well.

· The U-velocity increases in the main channel and decreases in the vegetation as the vegetation density increases, resulting in the increase in the vertical and spanwise Reynolds stresses at the vegetation interface.

· The maximum velocity region of U-velocity is shifted toward the inner wave due to the pressure driven secondary flows over water depth.

· Streamwise convective term and the pressure gradient produce upward and downward motions at the interface of the main channel and the vegetation zone.

· The present numerical model with conventional approach to detect the presence of vegetation can predict the flow structure for submerged vegetation satisfactorily, with some discrepancy in case of emergent vegetation. This infers that another set of model coefficients, C_{fk} and $C_{f\varepsilon}$ is needed for better agreement with the measurement for emergent vegetation. This limitation has been overcome by introducing new source/sink term in transport equations. Hence Approach 2 can be used for wide variety of flow filed with vegetation without any implementation of drag related model coefficients.

REFERENCES

Burke, R.W., Stolzenbach, K.D. 1983. Free surface flow through salt marsh grass. MIT-Sea Grant MITSG 83-16, Mass. Inst. of Technology, Cambridge, USA.

Choi, S., Kang, H. 2004. Reynolds stress modeling of vegetated open-channel flows. Journal of Hydraulic Research, Vol.42, No.1, pp.3-11.

Fischer-Antze, T., Stoesser, T., Bates, P.B., Olsen, N.R. 2001. 3D numerical modelling of open-channel flow with submerged vegetation. Journal of Hydraulic Research, Vol.39, No.3,pp.303-310.

Ghisalberti, M. 2007. The impact of submerged canopies on open channel hydrodynamics. Fifth International Symposium on environmental Hydraulics, Tempe, Arizona, USA.

Green, S.R. 1992. Modelling turbulent air flow in a stand of widely-spaced trees. PHOENICS Journal of Computational Fluid Dynamics and Application, Vol.5, pp. 294-312.

Jahra, F., Yamamoto, H., Tsubaki, R., Kawahara, Y. 2009. Experimental study of mean velocity distributions in open channels with emergent and submerged vegetation. Journal of Applied Mechanics, Vol.12, pp. 663-672.

James, C.S., Myers, W.R.C. 2001. Conveyance of meandering channel with marginal vegetation. Proceedings of the Institution of Civil Engineers. Water, Maritime and Energy, Vol.148, pp. 97-106.

Liu, J., Chen, J.M., Black, T.A., Novak, M.D. 1996. E-ε modelling of turbulent air flow downwind of a model forest edge. Boundary-Layer Meteorology, Kluwer Academic Publishers, Netherlands, Vol.77, pp.21-44.

Lopez, F., Garcia, M. 2001. Mean flow and turbulence structure of open-channel flow through non-emergent vegetation. Journal of Hydraulic Engineering, Vol.127, No.5, pp.392-402.

Lopez, F., Garcia, M. 1997. Open-channel flow through simulated vagetation: Turbulence modeling and sediment transport. Wetlands Res. Program Rep. WRP-CP-10, U.S. Army Corps of Engineers, Washington, D.C.

Poggi, D., Porporato, A., Ridolfi, L., Albertson, J.D., Katul, G.G. 2004. The effect of vegetation density on canopy sub-layer turbulence. Boundary-Layer Meteorology. Vol.111.pp.565-587.

Rodi, W. 1984. Turbulence models and their applications in hydraulics. A state-of-art review, International Association for Hydraulic Research, Delft, The Netherlands.

Shimizu, Y., Tsujimoto, T, 1994. Numerical analysis of turbulent open-chgannel flow over a vegetation layer using a k-ε turbulence model. Journal of Hydroscience and Hydraulic Engineering, Vol.11, No.2, pp.57-67.

Tsujimoto, T., Kitamura, T., Okada, T. 1991. Turbulent structure of flow over rigid vegetation-covered bed in open channels. KHL Progressive Rep.1, Hydr. Lab., Kanazawa Univerdity, Japan.
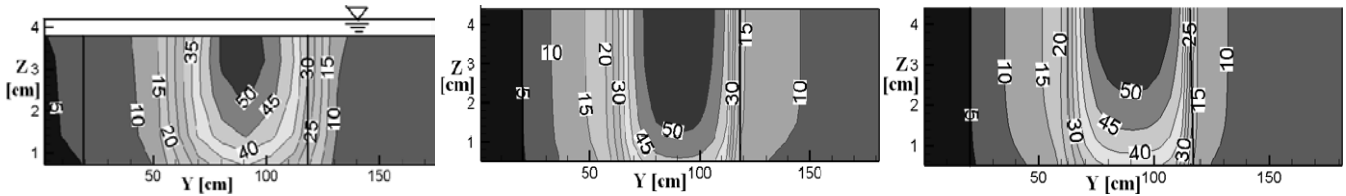
Figure 10(a). *U*-velocity (cm/sec) contour of emergent vegetation for Case B1, at section *S5*. Left: Experimental result, Middle: Calculated result of Approach1, Right: Calculated result of Approach 2.
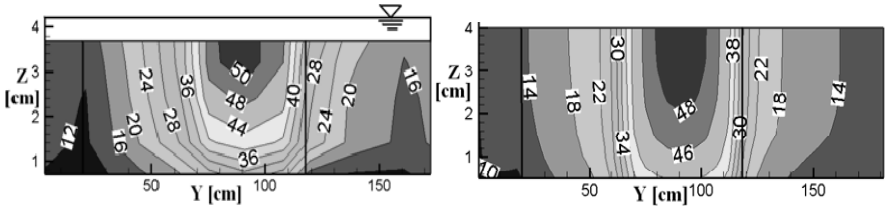

Figure 10(b). *U*-velocity (cm/sec) contour of emergent vegetation for Case B2, at section *S5*. Left: Experimental result, Middle: Calculated result of Approach1, Right: Calculated result of Approach 2.
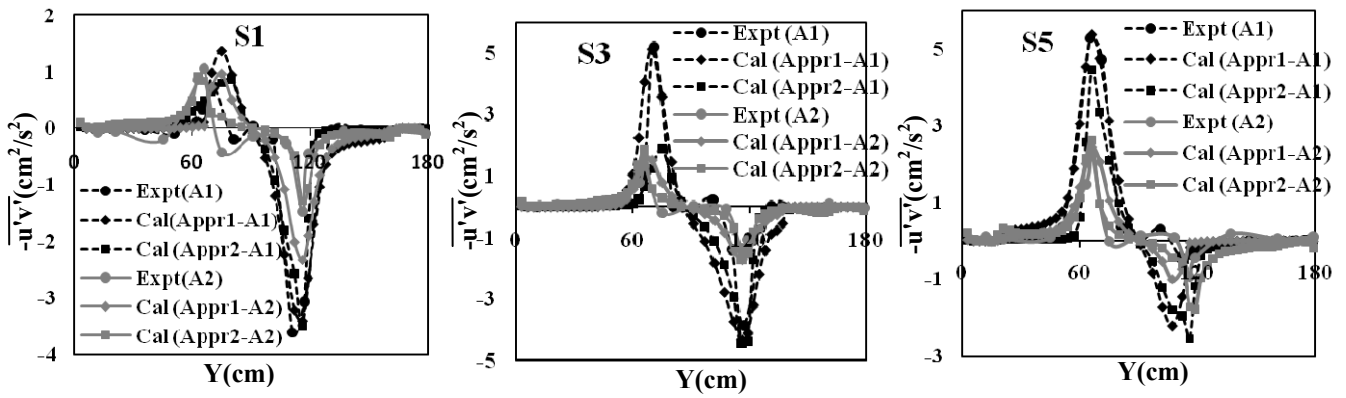

Figure 11 Experimental and calculated spanwise distribution of Reynolds stress profile for emergent vegetation.
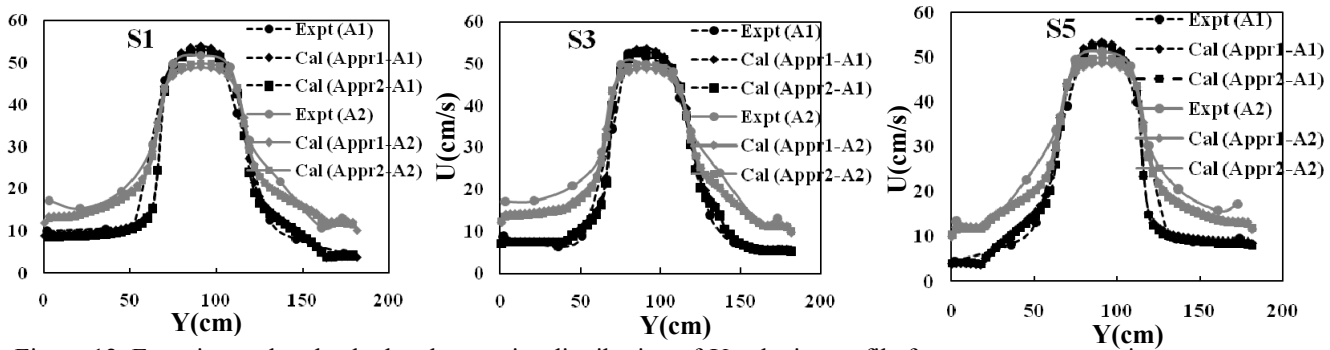

Figure 12. Experimental and calculated spanwise distribution of *U*-velocity profile for emergent vegetation.